International Journal of Automotive Technology, Vol. 17, No. 3, pp. 483–491 (2016)
DOI 10.1007/s12239–016–0050–9

pISSN 1229–9138/ eISSN 1976–3832

VEHICLE DISTANCE ESTIMATION USING A MONO-CAMERA FOR FCW/AEB SYSTEMS

J. HAN[1)], O. HEO[1)], M. PARK[1)], S. KEE[2)] and M. SUNWOO[3)*]

[1)]Electronics Dev. Team, Electronics Center, Mando Global R&D Center, 21 Pangyo-ro 255beon-gil, Bundang-gu, Seongnam-si, Gyeonggi 13486, Korea
[2)]Electronics Center, Mando Global R&D Center, 21 Pangyo-ro 255beon-gil, Bundang-gu, Seongnam-si, Gyeonggi 13486, Korea
[3)]Department of Automotive Engineering, Hanyang University, Seoul 04763, Korea

(Received 3 March 2015; Revised 26 July 2015; Accepted 28 November 2015)

ABSTRACT–For robust vision-based forward collision warning (FCW) and autonomous emergency braking (AEB) systems, not only reliable detection performance including high detection rate and low false positives but also accurate measurement output of a target vehicle is required. Especially, in order to reduce false alarm or activation of FCW/AEB systems, the systems require the precise measurement output of a target object, such as position, velocity, acceleration, and time-to-collision (TTC). In this study, we developed a measurement estimation algorithm of a target vehicle using a monocular camera. This method estimates two cases of vehicle widths for a target vehicle by using the detected lane information and a pin-hole camera model. After that, the position, velocity, acceleration, and TTC of a target vehicle are estimated by using a Kalman filter for the each estimated vehicle width. To improve robustness, the both estimation results using the detected lane information and the pin-hole camera model are fused. This estimation algorithm was evaluated and compared with the state-of-the-art technology. As a result, the proposed measurement output estimation method can improve the performance of the FCW/AEB systems.

KEY WORDS : Vehicle detection, Measurement output, Distance estimation, Time-to-collision (TTC), Camera

1. INTRODUCTION

Recently, various driver assistance systems (DAS) have been adopted for driving safety, such as a lane keeping assistance system (LKAS), a forward collision warning (FCW) system, and an autonomous emergency braking (AEB) system. Especially, FCW/AEB systems can help drivers to avoid or mitigate numerous accidents which are generally caused by late braking or insufficient braking force (Moon *et al*., 2012). Euro NCAP also decided to include AEB assessments as part of overall star rating from 2014. Most AEB systems identify potential collision by using radar sensors which have reliable detection performance at any type of weather. Compared to radar sensors, mono-cameras can be used for multiple applications including LKAS and AEB in low-cost. However, for robust vision-based FCW/AEB systems (Dagan *et al*., 2004; Raphael *et al*., 2011), not only a reliable detection performance including high detection rate and low false positives but also accurate measurement outputs of target vehicle is required. In particular, in order to false alarm or activation of FCW/AEB systems, the system requires the precise measurement output of a target object, such as position, velocity, acceleration, and time-to-collision (TTC) (Lee and Jeong, 2014).

In this study, we proposed a measurement estimation algorithm of a target vehicle using a monocular camera. The proposed estimation algorithm was evaluated and compared with the state-of-the-art technology (Stein *et al*., 2003, 2012) in a proving ground (PG) and normal roads. To evaluate measurement accuracy, a laser scanner was used for generating a ground truth (GT) data. As a result, the developed measurement output estimation method can improve the performance of the FCW/AEB systems.

The rest of this paper is organized as follows: First, background information of the measurement estimation is reviewed. Then, the overall algorithm structure is discussed. After that, two measurement estimation approaches are described. The fusion method of two estimation results is presented. Finally, experimental results are discussed comparing with the results of the state-of-the-art technology.

2. BACKGROUND

Typically, there are two types of methods to estimate distance of detected vehicles (Park and Hwang, 2014); one is using a vehicle image height and the other is using a vehicle image width. Both methods are based on a pin-hole camera model as in Figure 2. In Figure 2, a pin-hole camera model equation can be obtained by triangle formula as;

*Corresponding author. e-mail: msunwoo@hanyang.ac.kr

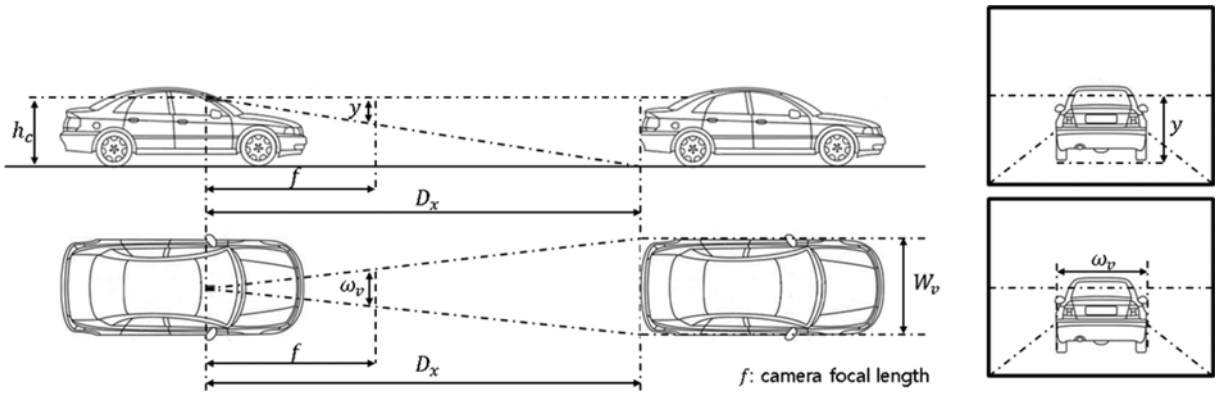

Figure 1. Distance estimation methods. Upper image describes the method using the vehicle image height and the lower image shows the method using the vehicle image width.

$$Oz = f\frac{Oy}{poy} \tag{1}$$

where f is the focal length, Oz is the object distance, Oy is the object height, and poy is the projected object height. From this pin-hole camera model, the vehicle distance can be measured.

2.1. Method Using Image Height

A method using a vehicle image height is described in Figure 1. From the pin-hole camera model, an equation of the method using a vehicle image height can be derived under assumption of plain roads as follows;

$$D_x = f\frac{h_c}{y} \tag{2}$$

where D_x is the longitudinal distance of the target vehicle, h_c is the camera height, and y is the vehicle image height between the horizon line and the bottom edge of the vehicle.

2.2. Method Using Image Width

A method using a vehicle image width is described in Figure 1. An equation of the method using vehicle image width can be derived by a pin-hole camera model as follow;

$$D_x = f\frac{W_v}{\omega_v} \tag{3}$$

where W_v is the vehicle physical width, and ω_v is the vehicle image width between left edge and right edge of the vehicle.

A vehicle distance should be estimated precisely even in the various road or driving conditions, as shown in Figure 3.

Therefore the two types of methods have its advantage and disadvantage described in Table 1. The method using image height requires the exact vehicle image height to detect the vehicle distance. However, due to the road condition and pitch motion of the ego-vehicle, the horizon line can be changed, as shown in Figure 3. In Figure 3, the vehicle image heights are different even the target vehicles are in same distance. In addition, the exact bottom edge of the vehicle in the image is hard to find at certain conditions, such as low sun, night, and rainy road. On the other hand, the method using image width does not need the vehicle

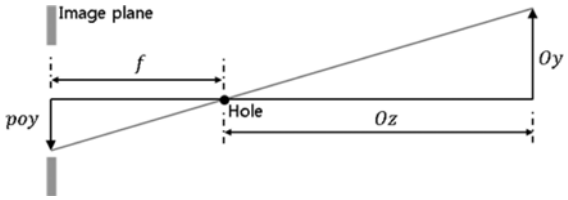

Figure 2. Pin-hole camera model.

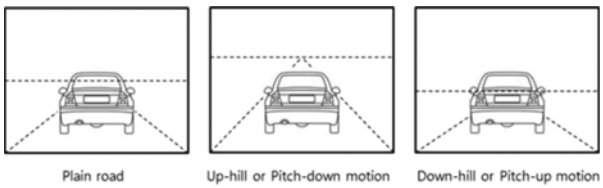

Figure 3. Various road or driving conditions.

Table 1. Comparison between methods using image height and width.

	Advantage	Disadvantage
Method 1 (using height)	No need to know vehicle width	Hard to find the exact vehicle image height - Horizon line is dependent of pitch motion and road condition
Method 2 (using width)	Robust to the pitch motion and road condition	Vehicle width is unknown - Vehicle width should be also estimated

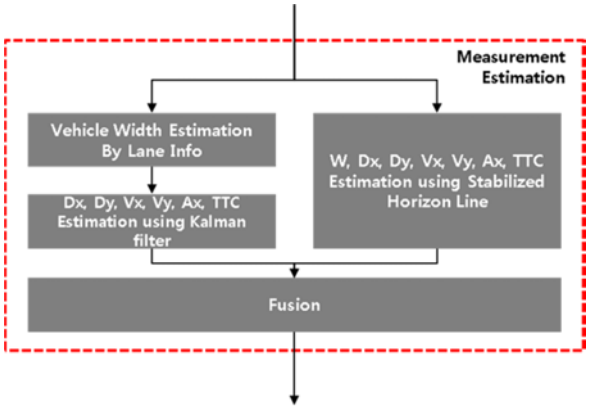

Figure 4. Overall algorithm structure of the measurement estimation.

image height. Thus the method is robust to the pitch motion and road condition for estimating the distance. However, in order to use the method using the image width, the vehicle width should be also correctly estimated.

3. OVERALL ALGORITHM STRUCTURE

In this study, the measurement signals including relative position, velocity, and acceleration of target vehicles were estimated by using the two approaches in Figure 4. First, the measurement signals were estimated by the vehicle image width. In this method, vehicle width was estimated by using the detected lane marking information, which can provide the robust vehicle width. The other approach also estimates the measurement signals by the vehicle width. However, in this method, the vehicle width was estimated by using the height of the image of the vehicle. This approach can estimate the measurement signals even though the detected lane markings are not valid. Finally, the estimation results of the measurement signals were generated by fusing the results of these two approaches.

4. ESTIMATION WITH LANE INFORMATION

Generally, a vehicle drives on a road which has both lane markings. If these lane markings can be detected precisely, the width of a target vehicle can be also accurately observed. Under assumption that the detected lane width is consistent within a certain range, the width of a target vehicle can be computed by proportional expression using a vehicle image width, a lane image width, and the detected lane width. If the lane detection result was not valid, the estimated width of the target vehicle is maintained because the vehicle width cannot be also changed. If a vehicle is first detected when both lane markings are not valid, the width of the target vehicle cannot be estimated by using the lane marking information until the lane detection result becomes valid. From the estimated vehicle width, longitudinal and lateral distances of the target vehicles were

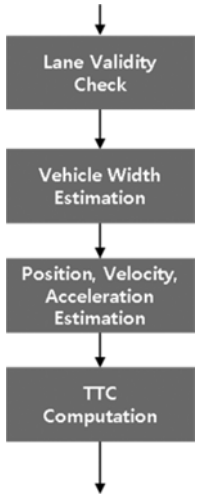

Figure 5. Overview of an estimation algorithm with lane information.

computed by a pin-hole camera model. After that, longitudinal position, velocity, and acceleration of the target vehicles were tracked by applying a Kalman filter with a constant acceleration model. Finally, the time-to-collision (TTC) value of the target vehicle was computed using its estimated position, velocity, and acceleration. Figure 5 describes the overview of the estimation algorithm with lane information.

4.1. Lane Validity Check

Lane detection algorithm generates both left and right cubic polynomial lane marking model parameters including other useful information, such as lane marking types, colors, quality, and view range. The quality of the detected lane markings specifies how accurate the detected lane makrings are. In addition, view range stands for the detected range of lane markings. In order to check the validity of the detected lane markings, these quality and view range signals were simply used as shown in Figure 6.

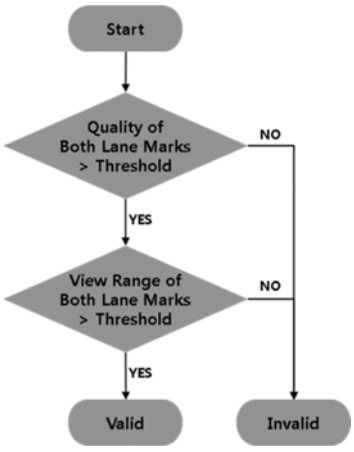

Figure 6. Lane validity check.

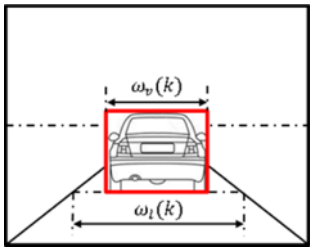

Figure 7. Vehicle width estimation using lane information.

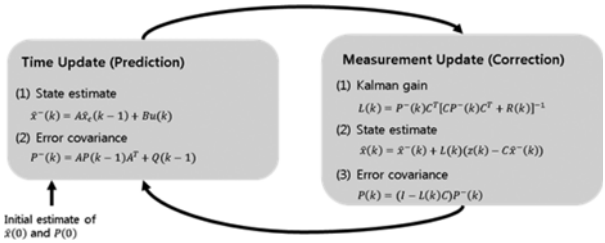

Figure 8. Kalman filter.

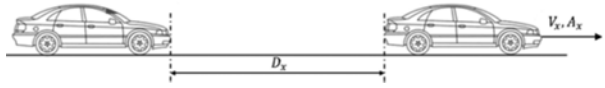

Figure 9. TTC computation.

4.2. Vehicle Width Estimation

In Figure 7, if the detected lane markings are valid, the width of the target vehicle is estimated by proportional expression as;

$$W_v(k) = \frac{\omega_v(k)}{\omega_l(k)} W_l(k) \tag{4}$$

where ω_l is the lane image width and $W_l(k)$ is the lane physical width between left and right lane markings.

4.3. Position, Velocity, and Acceleration Estimation

4.3.1. Constant acceleration model

In order to estimate the longitudinal position, velocity, and acceleration, the target vehicle is assumed to be moving in constant acceleration. Thus a constant acceleration model was designed as follows;

$$x(k+1) = Ax(k) + Bu(k)$$

$$= \begin{bmatrix} 1 & T & \frac{T^2}{2} \\ 0 & 1 & T \\ 0 & 0 & 1 \end{bmatrix} x(k-1) + Bu(k) \tag{5}$$

$$z(k) = Cx(k) = [1 \quad 0 \quad 0]x(k) \tag{6}$$

where state x equals $[D_x \; V_x \; A_x]^T$.

4.3.2. Kalman filtering

The longitudinal position, velocity, and acceleration were estimated by Kalman filters with the each constant acceleration model as shown in Figure 8. The longitudinal measurement output $z(k)$ of the Kalman filter was used as;

$$z(k) = D_x(k) = f\frac{W_v(k)}{\omega_v(k)} \tag{7}$$

In order to enhance the estimation performance, the longitudinal velocity can be also used to the measurement output. Then, the measurement output becomes a 2 × 1 matrix and the C matrix becomes a 2 × 3 matrix.

4.4. TTC Computation

In Figure 9, from the estimated longitudinal position, velocity, and acceleration of the target vehicle, TTC value was computed as follows;

$$TTC(k) = -\frac{D_x(k)}{V_x(k)},$$

$$\text{if } A_x(k) = 0 \;\; (\textit{Constant Velocity Model}) \tag{8}$$

$$TTC(k) = \frac{-V_x(k) - \sqrt{V_x^2(x) - 2A_x(k)D_x(k)}}{A_x(k)},$$

$$\text{if } A_x(k) \neq 0 \;\; (\textit{Constant Acceleration Model}) \tag{9}$$

where $0 \le TTC(k) \le TTC_{MAX}$. If the estimated acceleration value is equal to zero, the TTC value is calculated by a constant velocity model. Otherwise, the TTC value is obtained by a constant acceleration model.

5. ESTIMATION WITHOUT LANE INFORMATION

Even though there is a road which does not have both lane markings, vehicle width should be estimated to compute position, velocity, and acceleration of target vehicles in this study. To estimate vehicle width without lane information, an estimation result of horizon line was used. However, the estimation performance of the horizon line was also degraded when both lanes were not exist or invisible on the road. Therefore, the horizon line was tried to be estimated by using the detected vehicles and its width, if the lane detection result was not valid. Then the widths of target vehicles were estimated by using the horizon line and the bottom edge of the vehicle. The horizon line and vehicle width are recursively estimated using the information of each other. From the estimated vehicle width, longitudinal and lateral position of the target vehicles can be computed by a pin-hole camera model. After that, longitudinal position, velocity, and acceleration of the target vehicles were tracked by applying a Kalman filter with constant acceleration model. Finally, time-to-collision (TTC) values of the target vehicles were computed by using its estimated position, velocity, and acceleration. Figure 10 shows an overview of the estimation algorithm without lane information.

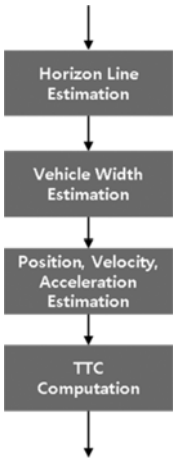

Figure 10. Overview of an estimation algorithm without lane information.

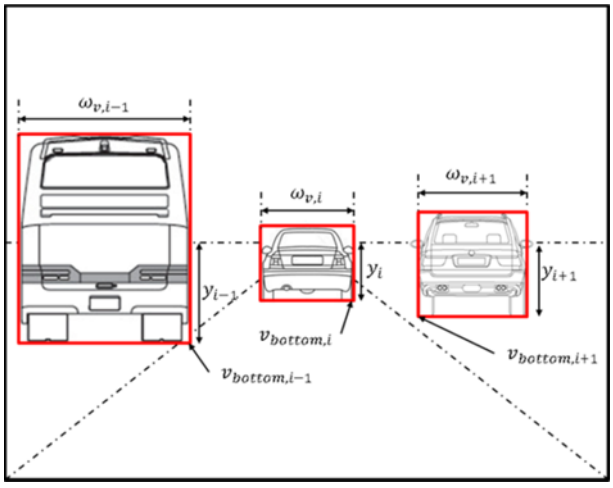

Figure 11. Horizon line estimation.

5.1. Horizon Line Estimation

If lane markings were valid, the horizon line was equal to the stabilized horizon line, which was computed in an image stabilization algorithm. On the other hand, if lane markings were not valid, the horizon line was estimated by the detected vehicles and its vehicle width. Simply, from the *i*-th vehicle bottom line $v_{\text{bottom,i}}$ and the *i*-th vehicle width $W_{\text{v,i}}$, the vehicle image height, y_{i} can be obtained by the a pin-hole camera model as shown in Figure 11. Thus, from the N number of the detected vehicles, the horizon line $v_{0,\text{VD}}$ can be computed by averaging its estimated horizon line as follows;

$$v_{0,\text{VD}} = \begin{cases} v_{0,\text{stabilized}}, & \textit{if Lane is valid} \\ \frac{1}{N}\Sigma_{\text{i}=1}^{\text{N}}\left(v_{\text{bottom,i}} - \frac{h_{\text{c}}}{W_{\text{v,i}}}\omega_{\text{v,i}}\right), & \textit{if Lane is not valid} \end{cases} \quad (10)$$

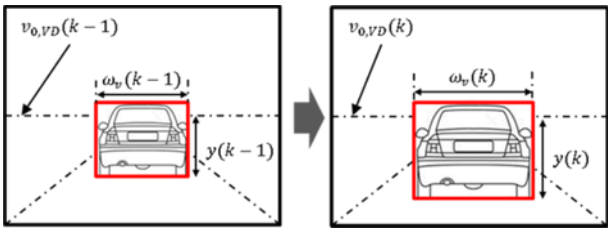

Figure 12. Vehicle width estimation.

5.2. Vehicle Width Estimation

5.2.1. Nonlinear vehicle width model

To estimate vehicle width, a nonlinear discrete model was designed by using a pin-hole camera model as shown in Figure 12. The model was designed as follows;

$$x(k) = f(x(k-1), \Delta\omega_{\text{v}}(k)) \quad (11)$$

$$z(k) = g(x(k)) \quad (12)$$

$$y(k) = y(k-1) + \frac{h_{\text{c}}}{W_{\text{v}}(k-1)}\Delta\omega_{\text{v}}(k) \quad (13)$$

$$W_{\text{v}}(k) = W_{\text{v}}(k-1) \quad (14)$$

where the state $x = [y, W_{\text{v}}]^{\text{T}}$ and the measurement output $z = [y, W_{\text{v}}]^{\text{T}}$.

5.2.2. Extended kalman filtering

The vehicle width was estimated by extended Kalman filtering as shown in Figure 13. In Figure 13, the matrix A and C are computed as follows;

$$A(k) = \frac{\partial}{\partial x}(f(x(k), \Delta\omega_{v}(k)))\Big|_{\text{x}=\hat{\text{x}}(\text{k})} \quad (15)$$

$$C(k) = \frac{\partial}{\partial x}(g(x(k)))\Big|_{\text{x}=\hat{\text{x}}(\text{k})} \quad (16)$$

5.3. Position, Velocity, and Acceleration Estimation

The longitudinal position, velocity, and acceleration were estimated by the same method as described in the estimation method using lane information.

5.4. TTC Computation

The TTC value was computed by Equations (8) and (9) as

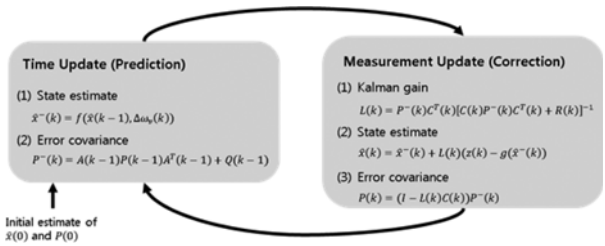

Figure 13. Extended kalman filter.

same as the estimation method with lane information.

6. FUSION OF MEASUREMENT ESTIMATION

Basically, if the detected lane markings were consecutively valid in a long time period, the estimation result of the method using the lane information had a good performance. However, the previous two measurement estimation results were fused for robust estimation result, because the detected lane markings were not always valid. Especially, the accuracy of the detected lane parameters was not good even though the lane markings are decided to be valid.

6.1. Reliability of Estimation Results with Lane

According to the estimation result of the vehicle width by the method using the lane information, the measurement score by the method with the lane information was decided. The estimation quality of the vehicle width can be measured by its standard deviation as shown in Figures 14 and 15. The reliability of the estimation result with lane information S was obtained by as follows;

$$S(k) = w_{\text{LANE}}\alpha(k)\frac{\sigma_{\text{MAX}}-\sigma(k)}{\sigma_{\text{MAX}}}, \text{ where } 0 \le S(k) \le 1 \quad (17)$$

$$\alpha(k) = \frac{c(k)}{c_{\text{MAX}}}, \text{ where } 0 \le \alpha(k) \le 1 \quad (18)$$

where σ is a standard deviation of vehicle width estimated by the method using lane, σ_{MAX} is a maximum sigma value as a tuning parameter, α is a maturity coefficient, c is a estimated time, c_{MAX} is a maximum estimated age as a tuning parameter, and w_{LANE} is a weight of estimation by the method using lane.

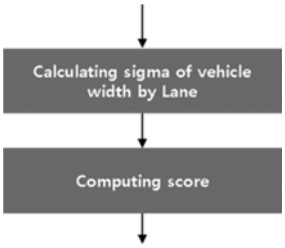

Figure 14. Score of estimation results with lane.

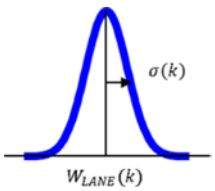

Figure 15. Sigma value of vehicle width by lane.

Figure 16. Laser scanner for the ground truth measurement.

Table 2. Specification of the laser scanner for generating GT data.

	Ibeo LUX 2010
Measurement range	Up to 200 m
Horizontal FOV	85°
Sampling rate	12.5 / 25.0 / 50 Hz
Accuracy	10 cm
Angular resolution	0.125°

6.2. Fusion of Estimation Results between with and without Lane

From the computed reliability score, the final measurement estimation results can be described as a weighted sum of the each estimation result as shown below;

$$D_{\text{x,fusion}}(k) = S(k)D_{\text{x,Lane}}(x) + (1-S(k))D_{\text{x,NoLane}}(x) \quad (19)$$

$$V_{\text{x,fusion}}(k) = S(k)V_{\text{x,Lane}}(x) + (1-S(k))V_{\text{x,NoLane}}(x) \quad (20)$$

$$A_{\text{x,fusion}}(k) = S(k)A_{\text{x,Lane}}(x) + (1-S(k))A_{\text{x,NoLane}}(x) \quad (21)$$

$$TTC_{\text{x,fusion}}(k) = \begin{cases} S(k)TTC_{\text{x,Lane}}(x) + (1-S(k))TTC_{\text{x,NoLane}}(x), \\ \quad \text{if } TTC_{\text{x,Lane}}(x) < TTC_{\text{MAX}} \text{ and } (x) < TTC_{\text{MAX}} \\ \min(TTC_{\text{x,Lane}}(x),\ TTC_{\text{x,NoLane}}(x)), \\ \quad \text{if } (x)TTC_{\text{MAX}} \text{ or } TTC_{\text{x,NoLane}}(x) = TTC_{\text{MAX}} \end{cases} \quad (22)$$

7. EXPERIMENTAL RESULTS

7.1. Experimental Setup

In order to evaluate accuracy of the measurement estimation results, a laser scanner was installed in a test vehicle with a front looking camera, as shown in Figure 16 and Table 2. This laser scanner can generate the accurate position and velocity of the target vehicle. Thus the data of the laser scanner was used for ground truth value of the estimation results. In addition, the state-of-the-art front looking mono camera was also mounted on the test vehicle to compare both estimation results.

7.2. Experimental Results

The proposed algorithm was evaluated on a PG and normal roads. In the PG, the test data was collected on roads with lane markings and roads without lane markings. In order to make the measurement estimation algorithm to be

independent of a vehicle detection algorithm, which finds a bounding box of target vehicles by image processing and generates the vehicle image width and height, the estimation results was evaluated by using two cases of the generated bounding boxes; one is manually detected vehicles and the other is detected by the vehicle detection algorithm. In this study, the estimation results of the closest-in-path-vehicle were only evaluated. The estimation results are presented as its means and 1 sigma values.

7.2.1. Evaluation results in PG

Overall evaluation results in the PG are shown in Tables 3 ~ 5. The state-of-the-art technology shows a very good performance of position and velocity estimation results in Table 3. However, the TTC error is larger than the error of our proposed algorithm with manually detected vehicles. In this case, the TTC error of the state-of-the-art technology was high because of a poor estimation performance of acceleration of the target vehicle even though it had good estimation result of both position and velocity (Stein *et al*., 2012, 2013). Figure 17 shows an example of the estimated TTC value with a vehicle detection algorithm. This test scenario was that the test vehicle was closing to the stopped target vehicle at constant speed and then the test vehicle was avoided a collision by steering change. In the most of the test cases, the TTC estimation results of our proposed algorithm were more stable and accurate than the results of the state-of-the-art technology. Especially, the TTC estimation performance is important because FCW/AEB systems generally decide collision risk by the TTC value. Moreover, our proposed algorithm with manually detected vehicles had a comparable performance of position and velocity estimation. However, in the case of estimation results with the vehicle detection algorithm, the estimation

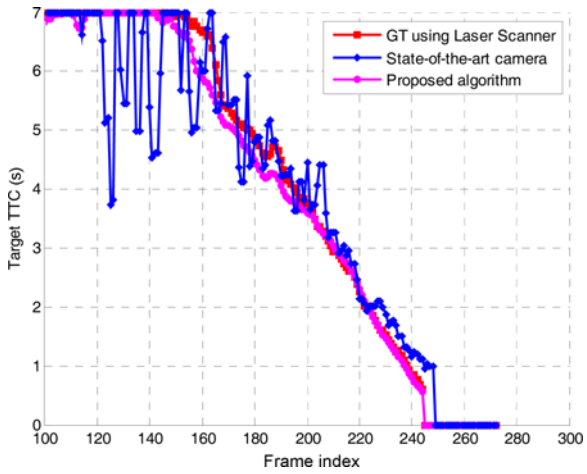

Figure 17. Example of TTC estimation results in PG.

Table 3. PG test results of the state-of-the-art technology (mean / 1 sigma).

		0 m ~ 45 m	45 m ~ 90 m	> 90 m
Long. position error		– 0.2 % / 4.2 %	– 1.5 % / 1.7 %	– 6.6 % / 3.8 %
Lat. position error		– 0.12 m / 0.15 m	– 0.18 m / 0.11 m	– 0.16 m / 0.28 m
	GT	0 m ~ 45 m	45 m ~ 90 m	> 90 m
Long. velocity error	6 m/s ~ 10 m/s	0.24 m/s / 0.37 m/s	0.55 m/s / 0.44 m/s	1.29 m/s / 0.38 m/s
	> 10 m/s	– 0.2 % / 4.2 %	– 4.7 % / 6.7 %	– 1.4 % / 16.8 %
TTC error – below 4 s		– 0.20 s (– 11 %) / 0.52 s (21 %)		

Table 4. PG test results of the proposed algorithm with a manually detected vehicle (mean / 1 sigma).

		0 m ~ 45 m	45 m ~ 90 m	> 90 m
Long. position error		2.9 % / 6.6 %	0.59 % / 5.4 %	3.9 % / 3.5 %
Lat. position error		0.09 m / 0.15 m	0.16 m / 0.11 m	0.30 m / 0.27 m
	GT	0 m ~ 45 m	45 m ~ 90 m	> 90 m
Long. velocity error	6 m/s ~ 10 m/s	– 0.14 m/s / 0.32 m/s	– 0.27 m/s / 0.96 m/s	– 1.03 m/s / 1.79 m/s
	> 10 m/s	2.9 % / 6.5 %	6.5 % / 10.2 %	4.5 % / 11.4 %
TTC error – below 4 s		– 0.07 s (0 %) / 0.39 s (12 %)		

Table 5. PG test results of the proposed algorithm with a vehicle detection algorithm (mean / 1 sigma).

		0 m ~ 45 m	45 m ~ 90 m	> 90 m
Long. position error		– 6.8 % / 7.1 %	– 6.5 % / 4.6 %	– 1.8 % / 4.8 %
Lat. position error		0.03 m / 0.24 m	0.19 m / 0.12 m	0.33 m / 0.26 m
	GT	0 m ~ 45 m	45 m ~ 90 m	> 90 m
Long. velocity error	6 m/s ~ 10 m/s	1.06 m/s / 1.02 m/s	– 0.72 m/s / 1.67 m/s	– 1.77 m/s / 2.81 m/s
	> 10 m/s	– 6.8 % / 7.1 %	5.0 % / 19.7 %	39.3 % / 24.2 %
TTC error – below 4 s		– 0.0 s (0 %) / 0.71 s (24 %)		

results had a poor performance because the proposed algorithm is highly dependent on the detected vehicle image width. Thus the detected vehicle image width should be also filtered or pre-processed before it becomes an input of the measurement estimation algorithm. In addition, the longitudinal position and velocity estimation performance on roads with no lane markings should be improved.

7.2.2. Evaluation Results in Normal Roads

Overall evaluation results in the normal roads are shown in Tables 6 ~ 8. As with the results in the PG, the estimation results of position and velocity of the state-of-the-art technology shows a remarkable performance of position and velocity estimation results in Table 6. However, its TTC error is also larger than the error of our proposed algorithm with manually detected vehicles. The TTC value of the state-of-the-art technology is seemed to be estimated by scale change of the detected bounding box for the target vehicle. Figure 18 shows an example of the estimated TTC value in a normal road with a vehicle detection algorithm. This test scenario was that the test vehicle was closing to the moving vehicle at high speed and then the test vehicle was braking near the target vehicle. In the most of the test cases, the TTC estimation results of our proposed

Table 6. Normal road test results of the state-of-the-art technology (mean / 1 sigma).

		0 m ~ 45 m	45 m ~ 90 m	> 90 m
Long. position error		4.5 % / 2.9 %	1.1 % / 4.4 %	– 4.8 % / 0.4 %
Lat. position error		– 0.12 m / 0.10 m	– 0.18 m / 0.32 m	– 0.46 m / 0.34 m
	GT	0 m ~ 45 m	45 m ~ 90 m	> 90 m
Long. velocity error	0 m/s ~ 6 m/s	0.06 m/s / 0.36 m/s	– 0.13 m/s / 0.78 m/s	0.00 m/s / 0.49 m/s
	6 m/s ~ 10 m/s	– 0.50 m/s / 0.37 m/s	– 0.38 m/s / 1.13 m/s	-
	> 10 m/s	4.49 % / 2.93 %	2.82 % / 2.35 %	-
TTC error – below 4 s		– 0.25 s (– 7 %) / 0.83 s (24 %)		

Table 7. Normal road test results of the proposed algorithm with a manually detected vehicle (mean / 1 sigma).

		0 m ~ 45 m	45 m ~ 90 m	> 90 m
Long. position error		– 1.3 % / 5.7 %	2.2 % / 6.8 %	– 3.7 % / 1.0 %
Lat. position error		0.04 m / 0.13 m	0.12 m / 0.31 m	– 0.11 m / 0.28 m
	GT	0 m ~ 45 m	45 m ~ 90 m	> 90 m
Long. velocity error	0 m/s ~ 6 m/s	– 0.37 m/s / 0.48 m/s	– 0.32 m/s / 0.72 m/s	– 2.18 m/s / 1.03 m/s
	6 m/s ~ 10 m/s	– 0.47 m/s / 0.44 m/s	– 0.04 m/s / 1.17 m/s	-
	> 10 m/s	– 1.3 % / 5.7 %	6.1 % / 3.2 %	-
TTC error – below 4 s		– 0.16 s (– 5 %) / 0.46 s (13 %)		

Table 8. Normal road test results of the proposed algorithm with a vehicle detection algorithm (mean / 1 sigma).

		0 m ~ 45 m	45 m ~ 90 m	> 90 m
Long. position error		3.1 % / 4.3 %	1.3 % / 5.3 %	– 9.2 % / – 2.2 %
Lat. position error		0.04 m / 0.13 m	0.16 m / 0.31 m	– 0.07 m / – 0.29 m
	GT	0 m ~ 45 m	45 m ~ 90 m	> 90 m
Long. velocity error	0 m/s ~ 6 m/s	– 0.01 m/s / 0.51 m/s	– 0.42 m/s / 1.54 m/s	– 8.68 m/s / 3.60 m/s
	6 m/s ~ 10 m/s	0.06 m/s / 1.05 m/s	– 1.68 m/s / 2.24 m/s	-
	> 10 m/s	3.1 % / 4.3 %	– 3.3 % / 11.7 %	-
TTC error – below 4 s		– 0.15 s (– 4.8 %) / 1.22 s (38 %)		

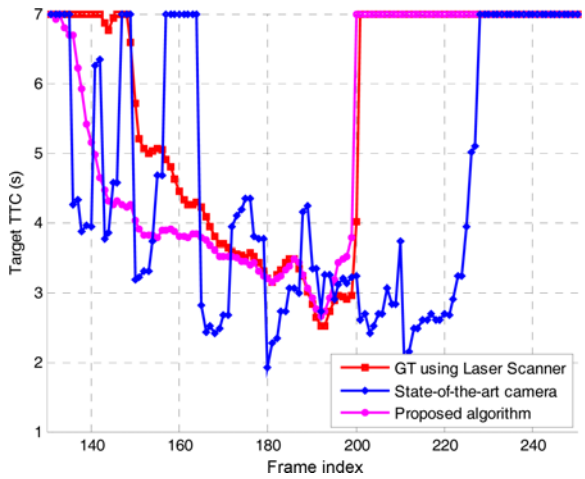

Figure 18. Example of TTC estimation results in normal roads.

algorithm were more stable and accurate than the results of the state-of-the-art technology. In particular, the braking should be activated in the most of the test scenarios in the normal roads. Therefore, if it was a real situation, FCW/AEB systems with our proposed algorithm could have a better system performance than with the state-of-the-art. In addition, our proposed algorithm with manually detected vehicles had comparable estimation performance of position and velocity. However, in the case of estimation results with the vehicle detection algorithm, the estimation results also had a poor performance because of the problem of the change of the vehicle image width. Consequently, the detected vehicle image width should be improved and stable by a preprocessing algorithm.

8. SUMMARY/FUTURE WORKS

In this study, we developed a measurement estimation algorithm of target vehicles including position, velocity, acceleration, and TTC. For a robust vision-based FCW/AEB system, the measurement accuracy as well as the vehicle detection performance is important. As experimental results, our proposed algorithm can have a comparable performance with the state-of-the-art technology and a better performance in the case of the TTC estimation results. However, to be the best technology of the measurement estimation, the following improvement should be achieved.

(1) Preprocessing or vehicle detection algorithm regarding the scale change of the vehicle image width should be improved. The more accurate bounding boxes of target vehicles guarantee the more accurate measurement estimation results.
(2) Measurement estimation algorithm on roads without lane marking should be improved. Precise measurement output is always required regardless of existence of lane marking.
(3) Amount of evaluation data and various test scenarios should be collected and evaluated. Reliable measurement estimation performance is necessary condition for vision-based FCW/AEB systems.

ACKNOWLEDGEMENT–This work was financially supported by the BK21 plus program (22A20130000045) under the Ministry of Education, Republic of Korea, by the National Research Foundation of Korea (NRF) grant funded by Ministry of Science, ICT and Future Planning (MSIP) of the Korea government (No. 2011-0017495), by the Industrial Strategy Technology Development Program of Ministry of Trade, Industry and Energy (No. 10039673), by the Industrial Strategy Technology Development Program of Ministry of Trade, Industry and Energy (No. 10042633), by Energy Resource R&D program (2006ETR11P091C) under the Ministry of Knowledge Economy, Republic of Korea, and by the Industrial Strategic Technology Development Program (10060068, "Development of Next Generation E/E Architecture and Body Domain Unit for Automotive Body Domain) funded By the Ministry of Trade, Industry & Energy (MOTIE, Korea).

REFERENCES

Dagan, E., Mano, O., Stein, G. P. and Shashua, A. (2004). Forward collision warning with a single camera. *IEEE Intelligent Vehicles Symp*., 37–42.

Lee, M. and Jeong, H. (2014). Driver propensity characterization for different forward collision warning times. *Int. J. Automotive Technology* **15**, **6**, 927–936.

Moon, S., Moon, I. and Shin, K. (2012). Forward collision warning system based on radar driven fusion with camera. *Proc. AVEC*.

Park, K. and Hwang, S. (2014). Robust range estimation with a monocular camera for vision-based forward collision warning system. *The Scientific World J.*, **2014**, 1–9.

Raphael, E., Kiefer, R., Reisman, P. and Hayon, G. (2011). Development of a camera-based forward collision alert system. *SAE Paper No*. 2011-01-0579.

Stein, G. P., Mano, O. and Shashua, A. (2003). Vision-based ACC with a single camera: bounds on range and range rate accuracy. *IEEE Intelligent Vehicles Symp*., 120–125.

Stein, G. P., Ferencz, A. D. and Avni, O. (2012). Estimating Distance to an Object Using a Sequence of Image Recorded by a Monocular Camera. US Patent. US 8,164,628.

Stein, G. P., Dagan, E., Mano, O. and Shashua, A. (2013). Collision Warning System. US Patent US 2013/0308828.